ADMET & DMPK **14** (2026) 3564*; doi: https://doi.org/10.5599/admet.3564*

ADMET

Open Access : ISSN : 1848-7718

http://www.pub.iapchem.org/ojs/index.php/admet

Original scientific paper

CRISPR/Cas12-powered electrochemical biosensor for chikungunya virus DNA detection using gold-modified screen-printed carbon electrodes

Clianta Yudin Kharismasari[1], Salma Nur Zakiyyah[2], Muhammad Ihda Hamlu Liwaissunati Zein[3], Ari Hardianto[1], Mara Mirasoli[3], Irkham[1,2,*] and Yeni Wahyuni Hartati[1,2★]

[1]*Department of Chemistry, Faculty of Mathematics and Natural Sciences, Universitas Padjadjaran, Sumedang 45363, Indonesia*

[2]*Study Center of Sensor and Green Chemistry, Faculty of Mathematics and Natural Sciences, Universitas Padjadjaran, Bandung 40132, Indonesia*

[3]*Department of Chemistry "Giacomo Ciamician", Alma Mater Studiorum - University of Bologna, Bologna 40126, Italy*

Corresponding Authors: E-mail: *irkham@unpad.ac.id; ★yeni.w.hartati@unpad.ac.id

Received: August 3, 2026; Revised: October 3, 2026; Published: October 27, 2026

Abstract

Background and purpose: Chikungunya virus (CHIKV) remains a health concern because its symptoms overlap with dengue and Zika, often leading to misdiagnosis. Conventional diagnostic methods, including viral isolation, enzyme-linked immunosorbent assay (ELISA) and reverse transcription-polymerase chain reaction (RT-PCR), are time-consuming, costly, and dependent on specialized laboratories. This study aimed to develop a rapid, selective, and sensitive electrochemical biosensor integrated with CRISPR/Cas12 for CHIKV DNA detection. **Experimental approach:** A CHIKV-specific guide RNA targeting a conserved region of the E1 gene was designed in silico and selected by specificity score (99.15) and E-value (1.7). The platform used a gold particle-modified screen-printed carbon electrode (SPCE/Au) functionalized with a ferrocene-labelled DNA reporter. The electrode was characterized electrochemically, and the biosensor was tested for its response to CHIKV DNA, its selectivity against dengue virus (DENV) and SARS-CoV-2, and its detection performance across target concentrations. **Key results:** Au deposition enhanced the electrochemical properties of the electrode. Recognition of CHIKV DNA activated the CRISPR/Cas12 complex, whose collateral cleavage of the reporter reduced the ferrocene oxidation signal. The biosensor exhibited a concentration-dependent response over 0.01 to 10 ppb, with a limit of detection of 0.92 ppb and a limit of quantification of 2.77 ppb. The biosensor showed excellent selectivity against CHIKV competitors. **Conclusion:** This work shows that combining CRISPR/Cas12 collateral cleavage with a ferrocene-labelled reporter on SPCE/Au enables rapid, selective, and sensitive CHIKV detection. Validation with clinical samples is still needed. The platform supports early diagnosis and disease surveillance, in line with Sustainable Development Goal (SDG) 3 (Good Health and Well-being).

©2026 by the authors. This article is an open-access article distributed under the terms and conditions of the Creative Commons Attribution license (http://creativecommons.org/licenses/by/4.0/).

Keywords

Arbovirus; collateral cleavage; electrochemistry; ferrocene signal; molecular diagnostics

Introduction

Chikungunya is a disease caused by the chikungunya virus (CHIKV), transmitted through the bite of *Aedes aegypti* and *Aedes albopictus* mosquitoes [1]. In 2025, Santos *et al.* [2] reported data on the classification of countries included in the endemic group (CHIKV circulates persistently in the region), the epidemic group

(CHIKV circulates sporadically in the region), and the no-transmission group (CHIKV does not circulate in the region). Chikungunya infection has been found in all tropical and subtropical countries worldwide, including Indonesia, which is in the epidemic group. Although chikungunya outbreaks in Indonesia are rare, climate change is changing the nature of mosquitoes (extrinsic incubation period), so it can increase the risk of transmission [2]. In Indonesia, Kejadian Luar Biasa/KLB (an epidemiological status marked by a sudden surge in cases, deaths, or disabilities in a specific area and period, with the potential to become an outbreak) of chikungunya still occurs periodically, and reports from the Ministry of Health of Indonesia state that the spread of this virus has the potential to increase along with the rainy season pattern [3].

The mortality rate for chikungunya in symptomatic patients is reported to be <0.1 %, indicating that the disease is not generally fatal. Only one in a thousand cases of chikungunya results in death. However, the risk of death may increase in the first three months after the onset [2,4]. Clinical symptoms of chikungunya include high fever (above 39 °C), nausea, headache, a red rash, muscle pain and joint pain (swelling) [1,2]. These symptoms are identical to those of DENV, the cause of dengue fever, and ZIKV, the cause of Zika virus. This presents a challenge in controlling CHIKV infection because misdiagnosis can occur if relying solely on clinical symptoms. Therefore, rapid and accurate laboratory detection is essential to support diagnosis and control the spread of the disease.

Virus isolation, ELISA and RT-PCR are available methods for detecting CHIKV. Virus isolation is a laboratory technique that separates and amplifies viruses from clinical samples for identification. This technique is useful for diagnostic purposes, but it requires a long processing time and is subject to potential viral growth failure due to contamination, sample characteristics, and sample storage [5,6]. ELISA is a serological testing technique that utilizes the specific interaction between an antigen and an enzyme-labelled antibody. This technique still has drawbacks, including low sensitivity, stability and specificity [7,8]. RT-PCR, a molecular diagnostic method, detects CHIKV DNA with high sensitivity and specificity. However, RT-PCR still has limitations, including high operational costs, the need for skilled personnel, and long processing times [9,10]. This limits early detection in areas with limited health facilities.

In recent years, electrochemical biosensors have become a promising alternative because of their speed, low sample requirements, and ease of miniaturization, which makes them portable. Electrochemical biosensors use bioreceptors tailored to the analyte biomolecule, enabling interaction that enhances detection sensitivity and selectivity [11]. In electrochemical biosensors, electrodes are vital components, playing a role in electron transfer and as a bioreceptor immobilization medium [12,13]. A screen-printed carbon electrode (SPCE) is a small electrode consisting of a carbon-based working electrode, a reference electrode, and an auxiliary electrode on a single inert substrate [14]. Carbon-based working electrodes offer characteristics suitable for use in a wide range of detection applications, such as low background current, a wide potential range, and inertness. However, these electrodes have limited conductivity and interaction with biomolecules. Therefore, SPCE must be modified before use in electrochemical biosensors [15].

Clustered regularly interspaced short palindromic repeats/CRISPR-associated 12 (CRISPR/Cas12) technology offers a new approach to molecular detection. The CRISPR/Cas12 system has a trans-cleavage activity capability that is specifically activated after recognizing and cutting a target DNA sequence. This specific target sequence recognition is guided by a short RNA molecule called sgRNA (single-guide RNA) so that the Cas12 protein can cut the desired DNA target [16]. Therefore, sgRNA must be designed so the CRISPR/Cas12 complex can specifically recognize the target nitrogen-base sequence, perform cis-cleavage of the target DNA, and then activate trans-cleavage of the surrounding single-stranded DNA. Trans-cleavage is used in electrochemical biosensors by cutting a DNA probe with an electrochemical indicator, so if trans-cleavage occurs due to the

(cc) BY

presence of the target, the resulting electrochemical signal is lower [17]. The integration of the CRISPR/Cas12 system with an electrochemical biosensor platform has the potential to produce a very fast, specific, and sensitive detection method [18-20].

Although CRISPR technology has been used in various biosensor platforms, research integrating it with electrochemical systems for CHIKV [21] detection is still limited. Previous research on CHIKV DNA detection using CRISPR/Cas12 by Bhardwaj *et al.* observed colour changes in solutions using fluorescence and lateral flow assay (LFA). However, these methods depend on lighting and individual interpretations [21]. Therefore, this study aimed to develop a CRISPR/Cas12-based electrochemical biosensor as a rapid, sensitive, specific, and selective detection method for CHIKV.

Experimental

Materials and reagents

The materials used in this research were aqua pro injection (PT Ikapharmindo Putramas), bovine serum albumin (BSA; Sigma Aldrich), Cas12a (New England Biolabs, Frankfurt am Main, Germany), chloroauric acid ($HAuCl_4$.$3H_2O$; Sigma Aldrich), DEPC treated water (Nippon Gene, Japan), DNA probe-Ferrocene (3'biotin-AAAAAAAAAAAAAAAAAAAA-5'Fc; Integrated DNA Technologies Pte Ltd., Singapore), DNA target (5'-GCATATTTAATAATGGCGACGCCCCCAAAGTCTG-3'; Integrated DNA Technologies Pte Ltd., Singapura), sgRNA (5'-UAAUUUCUACUCUUGUAGAUGGGGCGUCGCCAUUAUUAAA-3'; Integrated DNA Technologies Pte Ltd., Singapore), ethanol absolute (≥99.9 %, C_2H_6O; Merck), 1-(3-dimethylaminopropyl)-3-ethyl carbodiimide hydrochloride (EDC; Sigma Aldrich), magnesium chloride ($MgCl_2$; Sigma Aldrich), 3-mercaptopropionic acid (MPA; Sigma Aldrich), natrium chloride (NaCl Sigma Aldrich), N-hydroxysuccinimide (NHS; Sigma Aldrich), potassium chloride (KCl; Merck) nuclease-free water (NFW; HiMedia Laboratories Pvt Ltd., India), potassium ferricyanide ($[K_3[Fe(CN)_6]$; Sigma Aldrich), potassium ferrocyanide ($K_4[Fe(CN)_6]$; Sigma Aldrich), phosphate buffer saline pH 7.2-7.4 (PBS; FUJIFILM Wako, Japan), streptavidin (Promega), sulfuric acid (H_2SO_4; Merck), RNase inhibitor (Thermo Scientific, USA), Screen-printed carbon electrode consists of carbon-based working (diameter of 0.40 cm), carbon auxiliary electrodes, and silver as a reference electrode (Metrohm DropSens 110, Spain), and tris base.

Instrumentation

The instruments used were EmStat4X, which was connected to a computer using PSTrace 5.11 software (PalmSens, UK), scanning electron microscope (SEM, JEOL JCM-6000), incubator (JoanLab), pH meter (Mettler Toledo InLab), minicentrifuge (Thermo Scientific MicroCL 17R, USA), micropipette (DragonLab), microtube (Labselect), and micropipette tip.

DNA database of chikungunya virus

The sgRNA sequence was determined from the complete genome sequence of CHIKV that is available at the GenBank National Center of Biotechnology Information (NCBI) [22].

CRISPR/Cas12 single-guide RNA prediction

Identification of CHIKV-specific regions and sgRNA sequences for targeting the CRISPR/Cas12 system was carried out using the Benchling design tool [23] by examining the off-target scores.

Homology analysis of chikungunya virus competitors

The selected sgRNA candidates were analysed using BLAST to evaluate their specificity against their competitor viruses, namely Dengue and Zika, based on E values.

Modification of SPCE with gold

SPCE was washed with Aqua pro injection and dried, then dripped with 50 µL of 0.1 M H_2SO_4 and pretreated using cyclic voltammetry (CV) technique for 10 cycles with a potential range of 0.0 to 1.6 V, scan rate 0.1 V s^{-1} and potential step (E_{step}) 0.01 V. SPCE was rinsed with Aqua pro injection and dried, then added 50 µL of 1 mM $HAuCl_4$ and electrodeposited using chronoamperometry (CA) technique at a potential of -0.1 V for 100 seconds with a t interval of 0.1 seconds. Then, SPCE was rinsed again using Aqua pro injection and dried. SPCE/Au was dripped with 50 µL of 0.01 M $K_3[Fe(CN)_6]$ and 0.01 M $K_4[Fe(CN)_6]$ solutions in 0.1 M KCl to be characterized using differential pulse voltammetry (DPV) technique in the potential range of -0.3 to 0.5 V with a scan rate of 0.008 V s^{-1}; potential step 0.004 V; potential pulse 0.025 V, and t pulse 0.05 s. SPCE was also characterized by CV, electrochemical impedance spectroscopy (EIS) and scanning electron microscopy (SEM) [24,25].

Immobilization of ferrocene-labelled DNA probe (DNA probe-Fc)

SPCE/Au was washed with Aqua pro injection, then 3 µL of 0.01 M MPA was added and incubated for 20 minutes at room temperature. SPCE/Au was rinsed with ethanol:water (1:3, v/v) solution, dried, then 3 µL of EDC:NHS (1:1) solution was added and incubated for 60 minutes at room temperature. SPCE/Au was rinsed with Aqua pro injection and dried, then 3 µL of 50 ppm STV was added and incubated for 90 minutes at 4°C. SPCE/Au/STV was rinsed with 0.01 M PBS and dried, then 3 µL of 2 µM biotin-probe DNA-Fc was added and incubated for 60 minutes at room temperature. Next, the SPCE modified with the DNA probe was rinsed with 0.01 M PBS and dried. Finally, 0.01 % BSA was added to the SPCE and incubated for 10 minutes at room temperature. The modified SPCE was characterized using square wave voltammetry (SWV) over -0.1 to +0.5 V (0.004 V step, 0.025 V amplitude, 25 Hz frequency) in 0.01 M PBS to observe the ferrocene (Fc) oxidation signal [24].

Target recognition and cleavage by the CRISPR/Cas12-sgRNA complex

NFW, NEB buffer, Cas12a, and sgRNA were mixed into a microtube and incubated for 15 minutes at 37 °C, then mixed with the target DNA. The mixture solution containing the target DNA and the CRISPR/Cas12 complex was dropped onto a modified SPCE and incubated for 60 minutes at 37 °C. The electrode was rinsed with 0.01 M Tris-HCl pH 7.4 and allowed to dry. Next, 40 µL of 0.01 M PBS was added to the electrode and measured using SWV (potential range: 0.1 to +0.5 V; potential step: 0.004 V; amplitude: 0.025 V; frequency: 25 Hz) to measure the redox signal of the Fc label. The low Fc oxidation signal compared to the blank indicates that trans cleavage of the DNA probe by the CRISPR/Cas12 complex occurred.

Biosensor selectivity test

Three types of sample solutions containing CRISPR/Cas12 complexes were prepared, each targeting CHIKV RNA, DENV RNA, and SARS-CoV-2 DNA. All targets were at a concentration of 1 ppb. All sample solutions were tested on a CRISPR/Cas12-based electrochemical biosensor and measured using SWV. The resulting electrochemical response was compared with the current response of samples targeting CHIKV DNA.

Results and discussion

Design of single-guide RNA

CHIKV has a genome that encodes several genes for viral replication, including nonstructural (nsP1-nsP4) and structural (E1 and E2) proteins. Among these regions, the E1 and E2 genes are highly conserved and mutate less frequently, making them common targets for CHIKV detection. For example, a study by Zakiyyah *et al.* [26] targeted the highly specific E1 region of the CHIKV gene to detect CHIKV RNA using CRISPR/Cas13

(cc) BY

integrated with an electrochemical biosensor. In their study, they discovered a specific sequence belonging to CHIKV, namely 5'GGGGGCGUCGCCAUUAUUAAAUAU'3 [26].

In the CRISPR/Cas12 system, sgRNA is designed by combining a loop structure with a nitrogen base sequence (spacer) that will complement the target nitrogen base sequence. The loop structure is important for Cas protein binding, structural stabilization of the ribonucleoprotein complex, and activation of nuclease activity after target recognition [27-29]. One loop structure widely used in sgRNA design for the CRISPR/Cas12 system is AsCpf1 (UAAUUUCUACUCUUGUAGAU), synthesized from *Acidaminococcus sp.* [30]. Overall, sgRNA recognizes the target DNA strand through the target's PAM sequence (TTTN, where N is any nucleotide), then hybridizes with the DNA strand.

To design sgRNA, the CHIKV genome (NC_004162.2) was analysed to determine several candidate sequences based on their specificity (off-target) scores using the Benchling web tool. Table 1 contains the Benchling results and the top five candidate sequences. The cut position is the nucleotide position in the CHIKV genome where Cas12a is predicted to cut the target DNA, calculated automatically by Benchling based on the identified guide sequence and PAM locations. The strand indicates the DNA strand (+/−) where the target sequence is located, while the guide sequence is the 20-nucleotide (nt) protospacer sequence recognized by Cas12a.

Table 1. Candidate nitrogen base sequences for CHIKV sgRNAs of the CRISPR/Cas12 system. The (-) strand indicates the 3'-5' end, while the (+) strand indicates the 5'-3' end

No	Cut position	Strand	Guide sequence	PAM	Off-target score
1	426	+	CGCTACGGCGATGTCATGGG	TTTC	99.67
2	106	+	ACGGACATGTCATGCGAGGT	TTTA	99.54
3	155	+	GGGGCGTCGCCATTATTAAA	TTTG	99.15
4	133	-	ATAATGGCGACGCCCCCAAA	TTTA	99.10
5	286	+	TCGACGGCCTTGGCCAGCGC	TTTC	98.99

Benchling scans the input sequence for 20 nt protospacers located immediately upstream of a protospacer adjacent motif (PAM) on either strand. The PAM is a short DNA motif (2-6 nt) adjacent to the target sequence that is essential for target recognition and cleavage [31]. Candidate sequences were ranked by their off-target scores. Off-targeting is the binding of sgRNA and cleavage of non-target DNA sites that share partial complementarity with the guide. The off-target score in Benchling is an aggregated specificity score, obtained by comparing each candidate with potential off-target sites in the complete genome sequence of CHIKV (NC_004162.2) and penalizing sites with mismatches [32,33]. To minimize off-target effects, a high off-target value is chosen. In other words, the higher the off-target value, the more specific the nitrogen base sequence is to the target [24].

All candidates were analysed using BLAST to determine their specific similarity to CHIKV and its competitors, DENV (dengue) and ZIKV (zika) (Table 2). The level of similarity/homology of each candidate sequence can be seen from the *E*-value (expect value). The *E*-value is the number of alignments with an equal or better score that are expected to occur by chance in a database of a given size. It is calculated as $E = Kmne^{-\lambda S}$, where m and n are the lengths of the sequences being compared (in a database search, the query length and database size, respectively), *S* is the raw alignment score, *K* and λ are statistical parameters derived from the scoring system, and *e* is the base of the natural logarithm [34,35]. The smaller the *E*-value, the greater the similarity to a species [36]. Based on the data in Table 2, nitrogen base sequences number 2 and 3 tend to have the same level of homology with CHIKV, DENV and ZIKV. However, sequence number 3 was chosen as the target nitrogen base sequence because it is similar to the CHIKV-specific sequence identified by Zakiyyah *et al.* [26].

Table 2. BLAST analysis results of candidate sgRNA sequences. More than one value comes from different isolates of the same species

No	Guide sequence	*E* value		
		CHIKV	DENV	ZIKV
1	CGCTACGGCGATGTCATGGG	1.7	218	83; 326
2	ACGGACATGTCATGCGAGGT	1.7	218; 863	83; 326
3	GGGGCGTCGCCATTATTAAA	1.7	218; 863	83; 326
4	ATAATGGCGACGCCCCCAAA	1.7	55; 218; 863	326
5	TCGACGGCCTTGGCCAGCGC	1.7	218	82

The DNA nitrogen base sequence number 3 is converted into RNA and combined with the AsCpf1 loop structure to become a CHIKV DNA-specific sgRNA in the CRISPR/Cas12 system. When the sgRNA in the CRISPR/Cas12 complex recognizes the PAM of the target DNA, the spacer portion of the sgRNA will hybridize with the specific sequence of the target DNA through RNA-DNA interactions and the Cas12 protein will cut the target DNA (called cis-cleavage). After cis-cleavage, the complex is activated to perform trans-cleavage, which cuts the ssDNA surrounding the complex. The mechanism of action of the CRISPR/Cas12 complex in this study is illustrated in Figure 1.

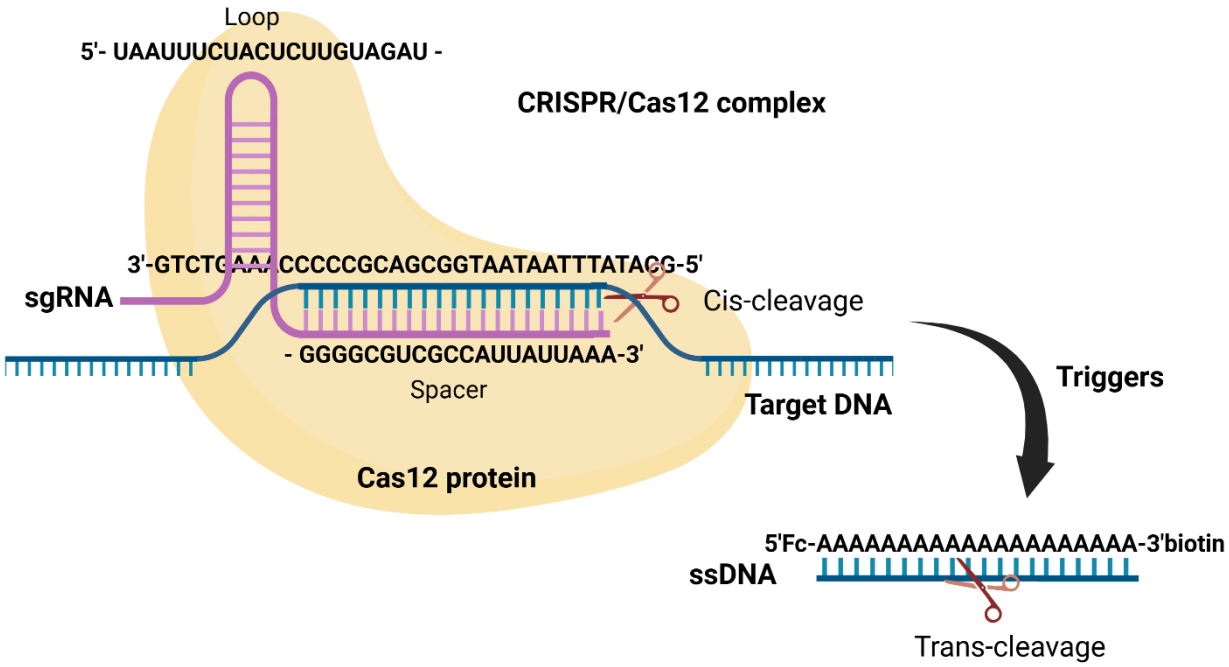


Figure 1. Illustration of sgRNA hybridization with CHIKV DNA and performing cis-cleavage so that trans-cleavage of the ssDNA probe can occur (Created with www.BioRender.com, accessed on January 5th, 2026)

Screen-printed carbon electrode modification with gold

Before electrodeposition, SPCE was pretreated with 50 µL of 0.1 M H_2SO_4 using CV for 10 cycles over 0.0 to 1.6 V at 0.1 V s^{-1} (0.01 V step). This treatment aims to clean the SPCE surface from contaminants contained in the carbon ink. This treatment increases the electroactive area of the SPCE, making the peak on the voltammetry curve more stable in the redox system $[Fe(CN)_6]^{3-/4-}$. H_2SO_4 solution effectively cleans the carbon electrode surface and makes it more hydrophilic by increasing carbon-oxygen functional groups (polar) [37,38]. With CV, the carbon surface can be oxidized at more positive potentials, creating oxygenated groups that reduce carbon hydrophobicity. That way, the aqueous metal precursor interacts more easily with the carbon surface [39].

The Au electrodeposition process was carried out by adding 50 µL of 1 mM $HAuCl_4$ and applying the CA technique at a fixed potential of -0.1 V for 100 s (t interval 0.1 s), so that the tetrachloroaurate ion ($AuCl_4^-$) underwent electrochemical reduction to solid gold (Au^0), which deposited on the surface of the SPCE carbon electrode [24]. Figure 2a shows an increase in the peak current height of the Au-modified SPCE in the

(cc) BY

$[Fe(CN)_6]^{3-/4-}$ system, indicating successful electrodeposition. Characterization was carried out by CV to determine the surface characteristics of the SPCE in the electrochemical system. Figure 2b shows that the Au-modified SPCE has a higher electron-transfer rate and peak current height in the $[Fe(CN)_6]^{3-/4-}$ system than the unmodified SPCE. Before modification, the SPCE had a peak oxidation-reduction potential difference of 0.21 V, while the Au-modified SPCE had 0.18 V. This indicates that the Au-modified SPCE achieved a faster electron-transfer rate because it required less energy to change from the oxidized to the reduced form.

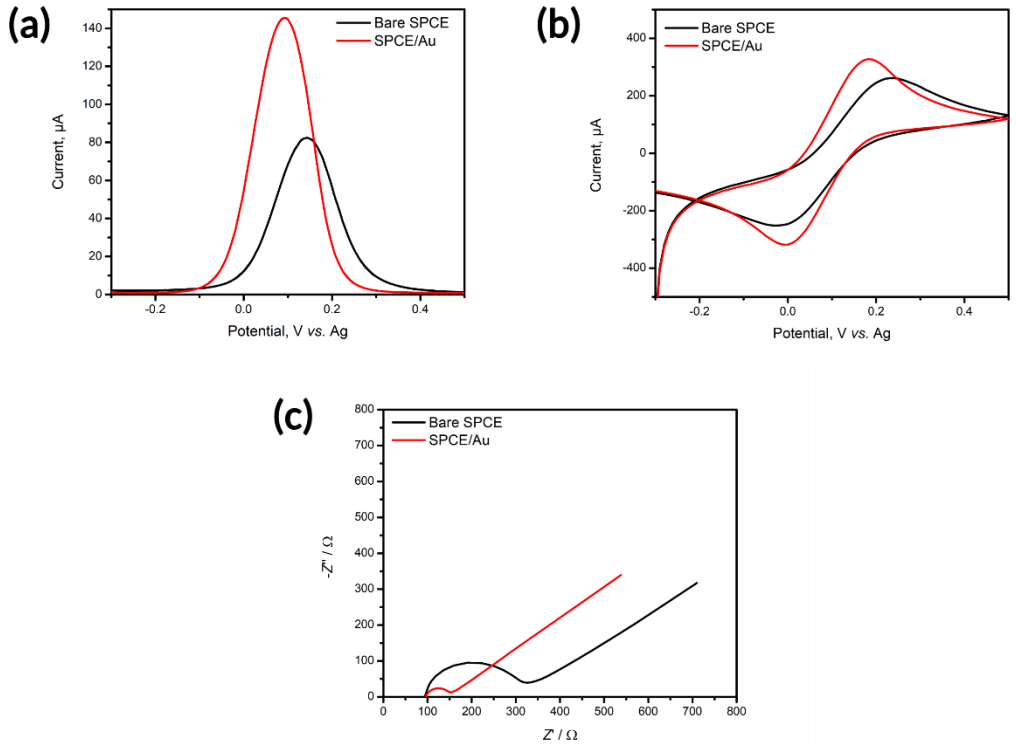


Figure 2. DPV voltammogram (a), CV voltammogram (b), and Nyquist plot EIS (c) of SPCE characterization before modification (black) and after Au modification (red) with $[Fe(CN)_6]^{3-/4-}$ redox system in 0.1 M KCl solution

Characterization was also carried out using EIS to determine the surface characteristics of SPCE based on its resistance. The Nyquist plot in Figure 2c shows that SPCE before modification has a larger semicircular diameter than SPCE after Au modification, indicating a higher charge-transfer resistance (R_{ct}). The R_{ct} value of SPCE before modification was 201.9 Ω, while it decreased to 43.95 Ω after Au modification. This decrease in the R_{ct} value indicates that Au modification effectively increases the conductivity of the electrode surface and accelerates the electron transfer process at the electrode-electrolyte interface. Au particles deposited on the SPCE surface enlarge the active surface area and reduce the kinetic resistance of the redox reaction. As a result, charge transfer becomes more efficient, reflected in the shrinkage of the semicircular diameter in the Nyquist plot.

SEM characterization was performed to observe the surface morphology of SPCE. Figures 3(a) and 3(b) and 3(c) and 3(d) show the SPCE surface before and after modification with Au. In Figures 3(c) and 3(d), white dots measuring approximately 0.2 to 0.3 µm represent Au particles attached to the SPCE surface. This indicates that the Au electrodeposition modification of the SPCE was successful.

The characterization was continued using EDX (energy-dispersive X-ray) to examine the composition of the SPCE surface. In Figure 4, the Au-modified SPCE surface shows three elements: carbon, oxygen, and Au. Carbon comes from the working electrode material on the SPCE, oxygen comes from oxidation of the SPCE surface during the pre-treatment process and Au comes from gold particles. The carbon, oxygen, and Au contents are 91.46±0.09 %, 6.59±0.09 % and 1.96±0.05 %, respectively.

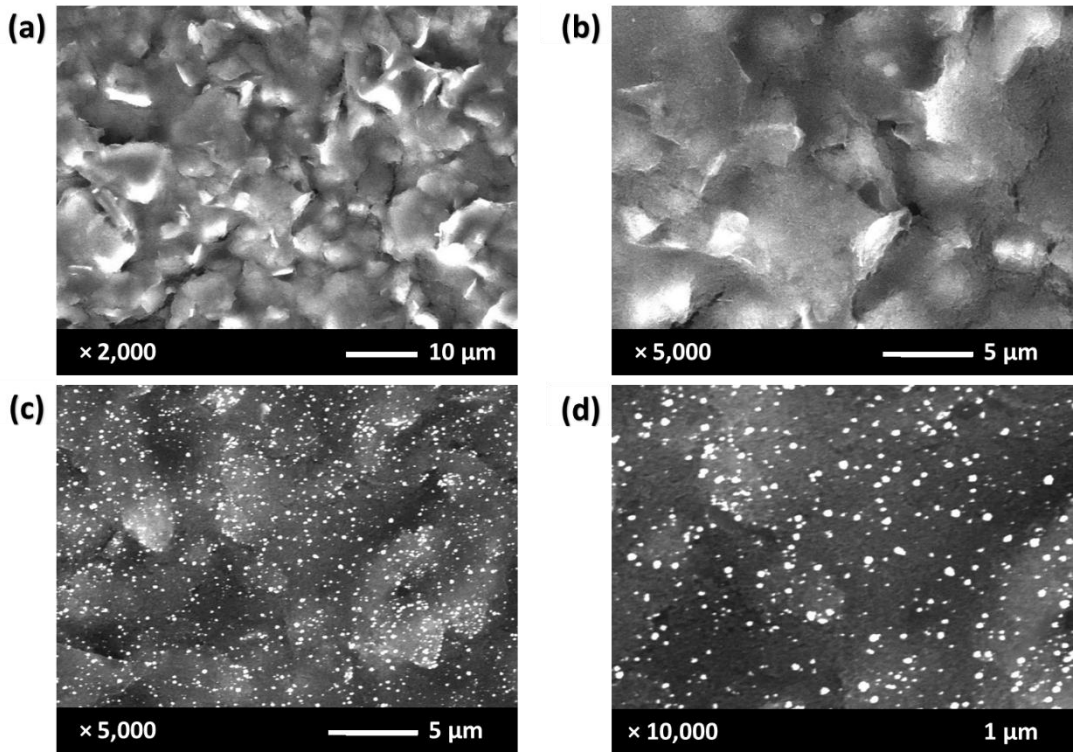


Figure 3. The results of SPCE surface characterization using SEM: a) bare SPCE 2; b) bare SPCE; c) SPCE/Au; d) SPCE/Au

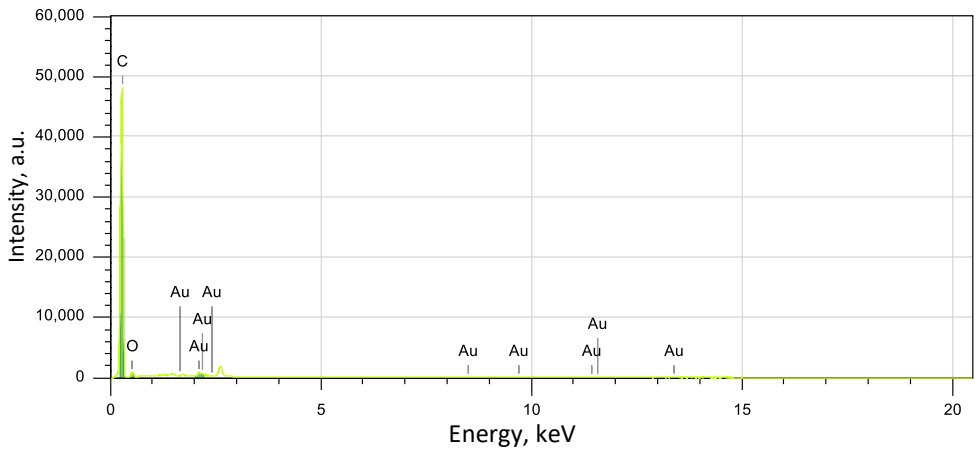


Figure 4. Characterization results of SPCE/Au using EDX

DNA probe immobilization on screen-printed carbon electode/Au using streptavidin-biotin system

SPCE/Au is supplemented with linkers in the form of MPA and EDC:NHS. MPA provides a carboxyl group that can be activated by EDC:NHS through a covalent (amide) bond. Au and MPA are covalently bonded through interactions between Au and thiols. EDC:NHS produces a reactive ester that reacts with the amine group in biomolecules, such as STV, forming a stable amide bond [24,40]. A DNA probe containing biotin and Fc as an electroactive indicator is immobilized on the SPCE surface through STV-biotin interaction. This interaction can occur due to the high affinity between STV and biotin (dissociation constant: ~10^{-14} M) [41]. BSA was added to prevent nonspecific reactions between the CRISPR complex and the electrode surface. The immobilization scheme of the DNA probe on the SPCE/Au surface is illustrated in Figure 5.

SWV characterization was performed using 0.01 M PBS solution as the electrolyte to determine the peak potential of Fc oxidation. In Figure 6, the Fc oxidation peak appears around +0.4 V, while the peak in the range of +0.1 to +0.2 V belongs to Au. This indicates that the DNA probe was successfully immobilized on the SPCE/Au surface.

(cc) BY

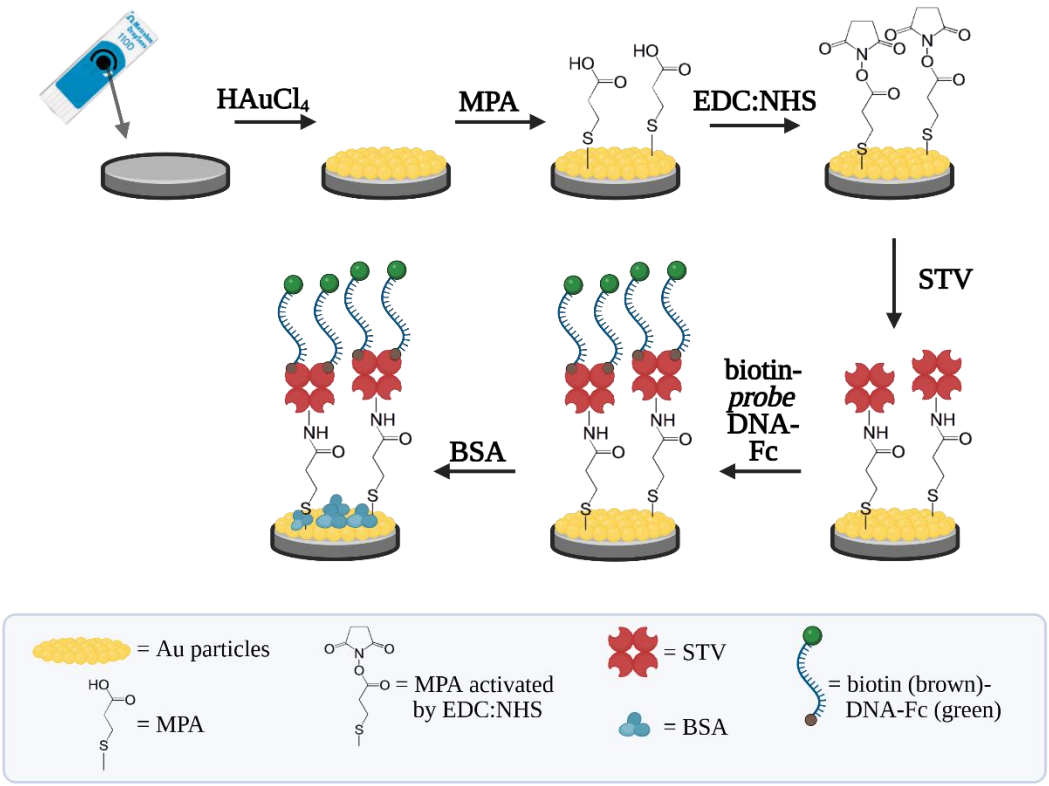


Figure 5. Illustration of modification of SPCE working electrode with gold and DNA probe (Created with www.BioRender.com accessed on May 13th, 2026)

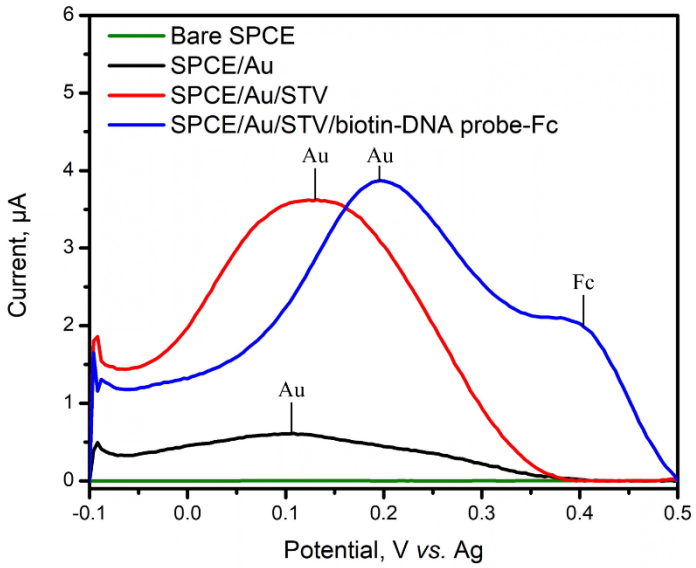


Figure 6. SWV voltammograms characterizing SPCE without modification (green), SPCE/Au (black), SPCE/Au/STV (red), and SPCE/Au/STV/biotin-probe DNA-Fc (blue) with the use of a linker. SWV potential range of -0.1 to +0.5 V; potential step 0.004 V; amplitude 0.025 V; and frequency 25 Hz, with 0.01 M PBS solution

We demonstrate the importance of the linker usage for DNA probe immobilization in Figure 7. Without the MPA/EDC:NHS linker, STV can only adsorb onto the Au surface through weak, non-covalent interactions between its amine groups and Au [42], rather than through the covalent amide bond described before. This weak attachment is insufficient to retain STV on the electrode surface during subsequent washing and measurement steps. Consequently, the biotinylated probe DNA-Fc, which is immobilized via STV-biotin interaction, is also not retained. No Fc oxidation peak is observed in the SWV response at +0.4 V (Figure 7), in contrast to the well-defined peak obtained when the linker is applied (Figure 6).

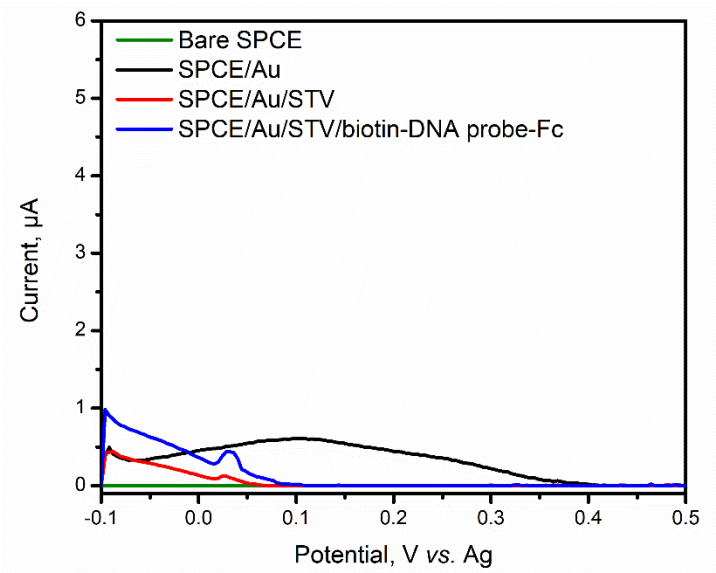


Figure 7. SWV voltammograms characterizing SPCE without modification (green), SPCE/Au (black), SPCE/Au/STV (red), and SPCE/Au/STV/biotin-probe DNA-Fc (blue) without the use of a linker. SWV potential range of -0.1 to +0.5 V; potential step 0.004 V; amplitude 0.025 V and frequency 25 Hz, with 0.01 M PBS solution

CRISPR/Cas12-based electrochemical biosensor performance

The mixed solution contains four components: NFW, NEB buffer pH 7.9, Cas12 (50 nM) and sgRNA (50 nM). NFW is nuclease-free water widely used to prepare biological test samples, especially those containing nucleic acids, because it prevents experimental failure from RNA or DNA degradation caused by nuclease enzymes (DNase and RNase). NEB buffer contains Mg^{2+} ions that play an important role in the conformational stability of the CRISPR/Cas12 complex. These ions also help facilitate the formation of the transition state required for DNA hydrolysis [43]. After the four components were mixed and incubated for 15 minutes at 37 °C, the target CHIKV DNA was added to the mixture and then immediately dropped onto the surface of the SPCE immobilized with the DNA probe. After 60 minutes of incubation at 37 °C, the SPCE was rinsed twice with 50 µL of 0.01 M Tris-HCl (pH 7.4) to maintain DNA probe stability, then measured by SWV in 0.01 M PBS.

The presence of a target in the sample can activate the CRISPR/Cas12 complex to trans-cleave the DNA probe that has been given an Fc indicator. As a result, the Fc oxidation peak height is lower compared to the sample without a target (blank). Figure 8 shows the difference in the Fc oxidation peak height in SPCE dripped with blank and target solutions. In this voltammogram, the graph was given a non-linear baseline treatment manually by determining the points considered baseline. This treatment aims to eliminate interfering signals, such as the Au signal at potentials of 0.1 to 0.2 V (as in Figure 6), so that only the Fc oxidation peak is displayed. The presence of target DNA can reduce the current peak height by up to 57%.

To assess the reproducibility of the blank sample test, measurements were performed on three independently fabricated SPCEs (n = 3). The average peak current obtained was 0.163 µA, with a relative standard deviation (RSD) of 4.25 %, indicating good reproducibility and confirming that the observed difference in peak current between the blank and target samples was not attributable to preparation-related variability.

CHIKV DNA detection testing was again conducted using varying target DNA concentrations to determine the effect of target concentration on the reduction of the Fc oxidation peak current. The CRISPR/Cas12 complex was allowed to interact with the target DNA and the immobilized DNA probe for 60 minutes at 37°C prior to SWV measurement. Target DNA samples were prepared at concentrations of 0.01, 0.1, 1 and 10 ppb (corresponding to 0.96, 9.61, 96.05 and 0.96 nM, respectively).

(cc) BY

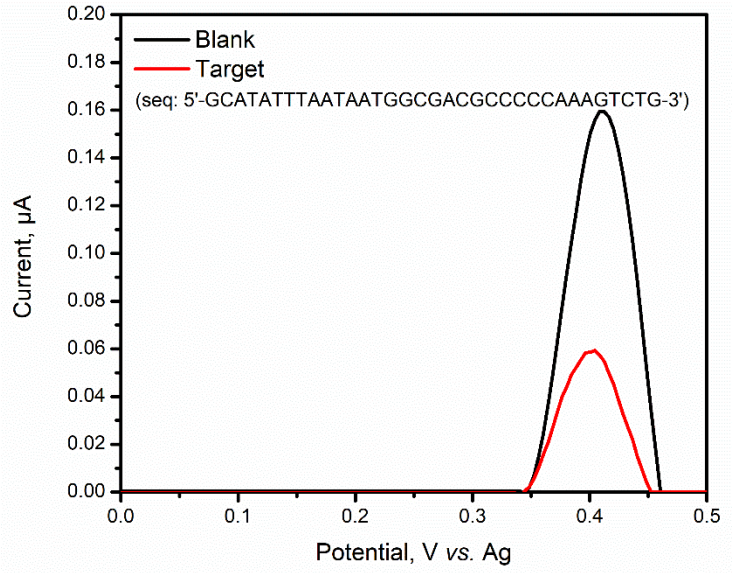


Figure 8. SWV voltammogram of CHIKV DNA detection against samples without target CHIKV DNA (black) and with target CHIKV DNA (red)

The results showed that the higher the target DNA concentration, the lower the Fc oxidation peak height (Figure 9). This indicates that the higher the target DNA concentration, the more DNA probe is cleaved. The present study did not investigate the effect of interaction time or ionic strength on the biosensor response. Systematic optimization of these parameters may further improve the sensitivity and reproducibility of the assay and is recommended for future work.

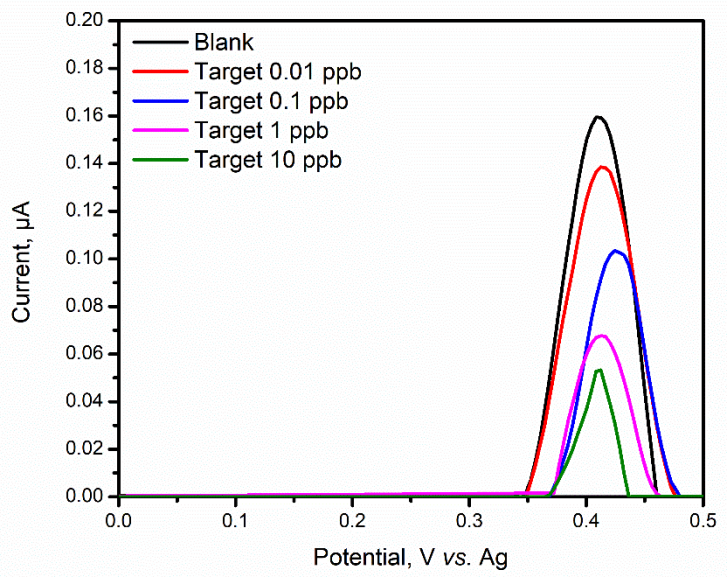


Figure 9. SWV voltammogram of CHIKV DNA detection concentration variation

To determine the LOD (limit of detection), LOQ (limit of quantification) and RSD, measurements of the blank and each target concentration were performed three times. The peak current height results obtained are listed in Table 3. The linear regression obtained is -0.0286x + 0.161 (R^2 = 0.9774) (Figure 10). The LOD and LOQ formulas used were based on ICH guidelines (3.3σ/slope for LOD, where σ is the standard deviation of the response) [44], so that the LOD obtained is 0.92 ppb (equivalent to 87.95 pM) and the LOQ obtained is 2.77 ppb (equivalent to 0.27 nM).

To further contextualize the performance of the developed CRISPR/Cas12-based biosensor, a comparison with previously reported electrochemical biosensors for CHIKV detection is summarized in Table 4.

Table 3. Peak current, average peak current and RSD of blank and target measurements

Target concentration, ppb	Current peak µA				RSD, %
	1st measurement	2nd measurement	3rd measurement	Average	
0.00 (blank)	0.160	0.173	0.157	0.163	4.25
0.01	0.138	0.123	0.131	0.131	4.69
0.10	0.103	0.109	0.110	0.107	2.88
1.00	0.068	0.059	0.066	0.064	5.99
10.00	0.053	0.055	0.053	0.054	1.76

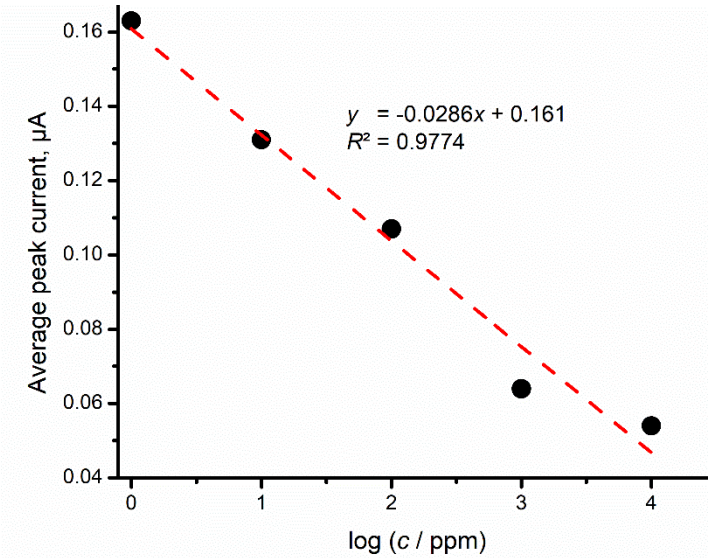


Figure 10. Calibration curve of the assay against the blank and target at varying concentrations. The concentration on the *x*-axis was expressed as log *c*, yielding integer values of 1, 2, 3 and 4 for the 0.01, 0.1, 1 and 10 ppb concentrations, respectively, while the blank was assigned *x* = 0 as a reference point (a convention adopted since a zero concentration has no defined logarithmic value). This transformation produced an *x*-axis with uniform, evenly spaced intervals for ease of interpretation

Table 4. Electrochemical biosensors for CHIKV detection

Recognition element/strategy, technique	Platform	Modification	Target	Linear range	LOD	Ref.
Lectin, EIS	Gold	ZnONp	Virion	Not explicitly stated	0.062 pfu mL^{-1}	[45]
Sandwich hybridization nano-conjugates, fluorescent/DPV	GCE	QDs-liposome @MB+Fe_3O_4	Protein E1 recombinant	10^{-14} to 10^{-8} g mL^{-1}	32.7 fg mL^{-1}	[46]
Antibody, EIS	Gold	SAM	Non-structural protein 3	25 - 1000 ng mL^{-1}	8 ng mL^{-1}	[47]
Antibody, EIS	SPCE	AuNP-PAni nanocomposite	Antigen	100 fg mL^{-1} -to 1 ng mL^{-1}	1.33 fg mL^{-1}	[48]
Aptamer, SWV	PCB	Au	Protein E1	5 pM - 100 nM	10 pM	[49]
Aptamer, CV & LSV	Carbon ink-printed	AgNP	Antigen	0.1 to 1000 ng mL^{-1}	0.1 ng mL^{-1}	[50]
Aptamer, CV	Origami-based ePAD	Ag-Au-ZnO	Antigen	1 to 10000 ng mL^{-1}	1 ng mL^{-1}	[51]
Antigen, EIS	Gold	Au-PAni-N,S-GQDs	Antibody	10 fg mL^{-1} to 1 ng mL^{-1}	22.1 fg mL^{-1}	[52]
DNA hybridization, CV	ePAD	Fe_3O_4@Au nanocubes	DNA	0.1 nM to 100 µM	0.1 nM	[53]
DNA hybridization, CV	SPGE	MoS_2 NSs	DNA	0.1 nM to 100 µM	3.4 nM	[54]
CRISPR/Cas13a, DPV	SPCE	Ceria	RNA	1 to 10,000 ppt	127 aM (1.325 ppt)	[26]
CRISPR/Cas12a (AsCpf1), SWV	SPCE	Au	DNA	0.96 pM to 0.96 nM (0.01 to 10 ppb)	87.95 pM (0.92 ppb)	This work

CRISPR/Cas12-based electrochemical biosensor selectivity

The selectivity of the CRISPR/Cas12a system for CHIKV DNA was evaluated by challenging the biosensor individually against each competitor nucleic acid, namely DENV RNA, CHIKV RNA (a related but non-target CHIKV sequence), and SARS-CoV-2 DNA, with each nucleic acid tested separately in its own reaction (*i.e.* not pooled into a single mixture) at a concentration of 1 ppb, matching the concentration used for the target

(cc) BY

CHIKV DNA to allow a direct and equivalent comparison. After each target/competitor incubation, the SPCE was rinsed twice with 50 µL of 0.01 M Tris-HCl pH 7.4 to remove unbound nucleic acids prior to SWV measurement. As shown in Figure 11, the Fc oxidation peak current (*I*) decreased significantly for CHIKV DNA (60.3 %), whereas the decreases for DENV RNA, CHIKV RNA and SARS-CoV-2 DNA were markedly lower at 15, 2.8 and 12.5 %, respectively. These results demonstrate that the CRISPR/Cas12a system exhibits good selectivity for CHIKV DNA over structurally related and clinically relevant competitor nucleic acids at an equivalent concentration.

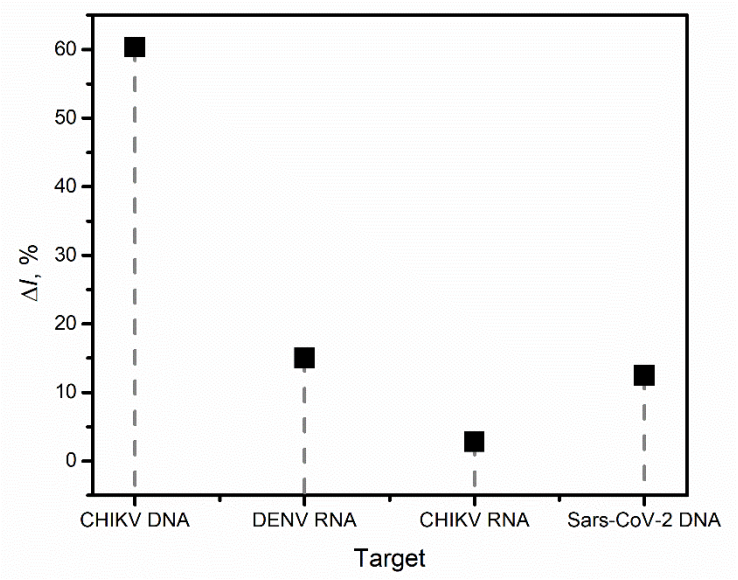


Figure 11. Selectivity test graph of the CRISPR/Cas12 system against CHIKV DNA and its competitors

Conclusions

This research successfully developed a rapid, sensitive, and selective electrochemical biosensor for CHIKV DNA detection integrated with the CRISPR/Cas12 system. The stages began with designing sgRNA specific to CHIKV DNA. The selected sgRNA sequence had an off-target score (specificity value) of 99.15 and an *E* value of 1.7, indicating specificity and high homology to CHIKV DNA. Modification of SPCE with Au, MPA and EDC:NHS linkers, and STV produced SPCE as a strong DNA-probe immobilization medium through STV-biotin interactions. The biosensor exhibited a linear response over a concentration range of 0.96 pM to 0.96 nM (0.01 to 10 ppb), with a limit of detection (LOD) of 87.95 pM (0.92 ppb) and a limit of quantification (LOQ) of 0.27 nM (2.77 ppb). In addition, the CRISPR/Cas12-based electrochemical biosensor had good selectivity to CHIKV DNA with a Δ*I* of 60.3 %.

Acknowledgements: *Yeni Wahyuni Hartati would like to thank Padjadjaran University and the Indonesian Endowment Fund for Education (LPDP) on behalf of the Indonesian Ministry of Higher Education, Science and Technology, managed under the EQUITY RMMP Program No. 4303/B3/DT.03.08/2025, 3927/UN6.RKT/HK.07.00/2025 and 4113/UN6.3.1/PT.00/2025.*

Conflict of interest*: Authors declare that there is no conflict of interest.*

CRediT authorship contribution statement*: All authors contributed to the study conception and design. Clianta Yudin Kharismasari: writing - original draft, data curation, formal analysis, investigation, visualization; Salma Nur Zakiyyah: Writing - review and editing, formal analysis, software; Muhammad Ihda Hamlu Liwaissunati Zein: writing - review and editing, methodology, visualization; Ari Hardianto: writing - review and editing, validation, supervision; Mara Mirasoli: writing - review and editing, validation, supervision; Irkham: writing - review and editing, conceptualization, resources, supervision; Yeni Wahyuni Hartati: writing - review and editing, conceptualization, funding acquisition, resources, supervision.*

References

[1] A.A. Bettis, M.L. Jackson, I.-K. Yoon, J.G. Breugelmans, A. Goios, D.J. Gubler, A.M. Powers. The global epidemiology of chikungunya from 1999 to 2020: A systematic literature review to inform the development and introduction of vaccines. *PLOS Neglected Tropical Diseases* **16** (2022) e0010069. https://doi.org/10.1371/journal.pntd.0010069

[2] H. Kang, A. Lim, M. Auzenbergs, A. Clark, F.J. Colón-González, H. Salje, H. Clapham, J.P. Carrera, J.-H. Kim, M. Malarski, S. López-Vergès, Z.M. Cucunubá, T. Cerqueira-Silva, W.J. Edmunds, S. Sahastrabuddhe, O.J. Brady, K. Abbas. Global, regional and national burden of chikungunya: force of infection mapping and spatial modelling study. *BMJ Global Health* **10** (2025) e018598. https://doi.org/10.1136/bmjgh-2024-018598

[3] Ministry of Health of the Republic of Indonesia. Laporan Mingguan Situasi Penyakit Infem dan Potensial KLB Wabah M42 2025 [Weekly Report on the Situation of Emerging Infectious Diseases and Potential Outbreaks, Week 42, 2025]. (2025). https://surveilans.kemkes.go.id/berita/laporan-mingguan-situasi-penyakit-infem-dan-potensial-klb-wabah-m42-2025 (in Indonesian; accessed November 11, 2025)

[4] G. Ribeiro dos Santos, F. Jawed, C. Mukandavire, A. Deol, D. Scarponi, L.E.G. Mboera, E. Seruyange, M.J.P. Poirier, S. Bosomprah, A.O. Udeze, K. Dellagi, N. Hozé, J. Chilongola, G.K. Nasrallah, S. Cauchemez, H. Salje. Global burden of chikungunya virus infections and the potential benefit of vaccination campaigns. *Nature Medicine* **31** (2025) 2342-2349. https://doi.org/10.1038/s41591-025-03703-w

[5] M. Kennedy. Methodology in diagnostic virology. *Veterinary Clinics of North America - Exotic Animal Practice* **8** (2005) 7-26. https://doi.org/10.1016/j.cvex.2004.09.009

[6] E.B. Martins, F. de Bruycker-Nogueira, C.D.S. Rodrigues, C.C. Santos, S.A. Sampaio, A.A. Fabri, V. Guerra-Campos, M.A.M. Mares-Guia, N.R.C. Faria, A.S. Santos, M.A.S. Pinto, M.F.B. Silva, I.C. V. Moraes, A. Pina-Costa, A.M.B. Filippis, P. Brasil, G.A. Calvet. Chikungunya virus shedding in semen: A case series. *Viruses* **14** (2022) 1879. https://doi.org/10.3390/v14091879

[7] G. Liu, J.F. Rusling. COVID-19 antibody tests and their limitations. *ACS Sensors* **6** (2021) 593-612. https://doi.org/10.1021/acssensors.0c02621

[8] C. Fischer, W.K. Jo, V. Haage, A. Moreira-Soto, E.F. de O. Filho, J.F. Drexler. Challenges towards serologic diagnostics of emerging arboviruses. *Clinical Microbiology and Infection* **27** (2021) 1221-1229. https://doi.org/10.1016/j.cmi.2021.05.047

[9] Y.-H. Shiao. A new reverse transcription-polymerase chain reaction method for accurate quantification. *BMC Biotechnology* **3** (2003) 22. https://doi.org/10.1186/1472-6750-3-22

[10] A. Andrew, T.N. Navien, T.S. Yeoh, M. Citartan, E. Mangantig, M.S.H. Sum, E.S. Ch'ng, T.-H. Tang. Diagnostic accuracy of serological tests for the diagnosis of Chikungunya virus infection: A systematic review and meta-analysis. *PLOS Neglected Tropical Diseases* **16** (2022) e0010152. https://doi.org/10.1371/journal.pntd.0010152

[11] S.N. Zakiyyah, Irkham, K.S.P. Sima, C.Y. Kharismasari, M. Xi, S. Gaffar, M. Ozsoz, F. Paolucci, G. Valenti, Y.W. Hartati. CRISPR-Cas13a-powered electrochemical biosensors for RNA-based disease diagnostic and monitoring. *Sensors and Actuators Reports* **10** (2025) 100358. https://doi.org/10.1016/j.snr.2025.100358

[12] I.H. Cho, D.H. Kim, S. Park. Electrochemical biosensors: perspective on functional nanomaterials for on-site analysis. *Biomaterials Research* **24** (2020) 6. https://doi.org/10.1186/s40824-019-0181-y

[13] A. Singh, A. Sharma, A. Ahmed, A.K. Sundramoorthy, H. Furukawa, S. Arya, A. Khosla. Recent advances in electrochemical biosensors: applications, challenges, and future Scope. *Biosensors* **11** (2021) 336. https://doi.org/10.3390/bios11090336

[14] W.T. Wahyuni, B.R. Putra, A. Fauzi, D. Ramadhanti, E. Rohaeti, R. Heryanto. A brief review on fabrication of screen-printed carbon electrode: materials and techniques. *Indonesian Journal of Chemical Research* **8** (2021) 210-218. https://doi.org/10.30598//ijcr.2021.7-wul

(cc) BY

[15] L.C. Chen, E. Wang, C.S. Tai, Y.C. Chiu, C.W. Li, Y.R. Lin, T.H. Lee, C.W. Huang, J.C. Chen, W.L. Chen. Improving the reproducibility, accuracy, and stability of an electrochemical biosensor platform for point-of-care use. *Biosensors and Bioelectronics* **155** (2020) 112111. https://doi.org/10.1016/j.bios.2020.112111

[16] C.Y. Kharismasari, Irkham, M.I.H.L. Zein, A. Hardianto, S. Nur Zakiyyah, A. Umar Ibrahim, M. Ozsoz, Y. Wahyuni Hartati. CRISPR/Cas12-based electrochemical biosensors for clinical diagnostic and food monitoring. *Bioelectrochemistry* **155** (2024) 108600. https://doi.org/10.1016/j.bioelechem.2023.108600

[17] M.I.H.L. Zein, C.Y. Kharismasari, A. Hardianto, S.N. Zakiyyah, R. Amalia, M. Ozsoz, M. Mirasoli, Irkham, Y.W. Hartati. A CRISPR/Cas12a electrochemical biosensing to detect pig mtDNA D-loop for ensuring food authenticity. *Sensing and Bio-Sensing Research* **47** (2025) 100755. https://doi.org/10.1016/j.sbsr.2025.100755

[18] W. Xu, T. Jin, Y. Dai, C.C. Liu. Surpassing the detection limit and accuracy of the electrochemical DNA sensor through the application of CRISPR Cas systems. *Biosensors and Bioelectronics* **155** (2020) 112100. https://doi.org/10.1016/j.bios.2020.112100

[19] C. Wu, Z. Chen, C. Li, Y. Hao, Y. Tang, Y. Yuan, L. Chai, T. Fan, J. Yu, X. Ma, O.A. Al-Hartomy, S. Wageh, A.G. Al-Sehemi, Z. Luo, Y. He, J. Li, Z. Xie, H. Zhang. CRISPR-Cas12a-empowered electrochemical biosensor for rapid and ultrasensitive detection of SARS-CoV-2 delta variant. *Nano-Micro Letters* **14** (2022) 159. https://doi.org/10.1007/s40820-022-00888-4

[20] Y. Lee, J. Choi, H.K. Han, S. Park, S.Y. Park, C. Park, C. Baek, T. Lee, J. Min. Fabrication of ultrasensitive electrochemical biosensor for dengue fever viral RNA Based on CRISPR/Cpf1 reaction. *Sensors and Actuators, B: Chemical* **326** (2021) 128677. https://doi.org/10.1016/j.snb.2020.128677

[21] P. Bhardwaj, S. Gulafshan, R. Singh. A rapid, specific and ultrasensitive detection of the Chikungunya virus based on RT-RPA:CRISPR/Cas12a one-pot dual mode end-point detection system. *Analytica Chimica Acta* **1329** (2024) 343221. https://doi.org/10.1016/J.ACA.2024.343221

[22] NCBI. Chikungunya virus, complete genome. https://ncbi.nlm.nih.gov/nuccore/NC_004162.2 (accessed May 18, 2024)

[23] Benchling. CRISPR Guide RNA Design Tool. https://www.benchling.com/crispr (accessed May 18, 2024)

[24] D.A. Wulandari, M.I.H.L. Zein, S.N. Zakiyyah, S. Ishmayana, M. Ozsoz, Y. Wahyuni Hartati, Irkham. CRISPR-Cas9-based electrochemical biosensor for the detection of *katG* gene mutations in isoniazid-resistant tuberculosis. *ADMET and DMPK* **13** (2025) 2766. https://doi.org/10.5599/admet.2766

[25] S. Zuliska, Irkham, S.N. Zakiyyah, Y.W. Hartati, Y. Einaga, I.P. Maksum. Electrochemical aptasensor for ultrasensitive detection of glycated hemoglobin (HbA1c) using gold-modified SPCE. *Sensing and Bio-Sensing Research* **47** (2025) 100765. https://doi.org/10.1016/j.sbsr.2025.100765

[26] S.N. Zakiyyah, Irkham, D.A. Wulandari, M.I.H.L. Zein, S. Gaffar, M. Ozsoz, G. Ogata, Y. Einaga, Y.W. Hartati. CRISPR-Cas13a-powered electrochemical biosensor for label-free detection of chikungunya virus RNA using a ceria-modified screen-printed carbon electrode. *ACS Sensors* **11** (2026) 923-938. https://doi.org/10.1021/acssensors.5c01924

[27] M. Jinek, K. Chylinski, I. Fonfara, M. Hauer, J.A. Doudna, E. Charpentier. A programmable dual-RNA-guided DNA endonuclease in adaptive bacterial immunity. *Science* **337** (2012) 816-821. https://doi.org/10.1126/science.1225829

[28] B. Zetsche, J.S. Gootenberg, O.O. Abudayyeh, I.M. Slaymaker, K.S. Makarova, P. Essletzbichler, S.E. Volz, J. Joung, J. Van Der Oost, A. Regev, E. V. Koonin, F. Zhang. Cpf1 is a single RNA-guided endonuclease of a class 2 CRISPR-Cas system. *Cell* **163** (2015) 759-771. https://doi.org/10.1016/j.cell.2015.09.038

[29] T. Yamano, H. Nishimasu, B. Zetsche, H. Hirano, I.M. Slaymaker, Y. Li, I. Fedorova, T. Nakane, K.S. Makarova, E. V. Koonin, R. Ishitani, F. Zhang, O. Nureki. Crystal structure of Cpf1 in complex with guide RNA and target DNA. *Cell* **165** (2016) 949-962. https://doi.org/10.1016/j.cell.2016.04.003

[30] L. Lin, X. He, T. Zhao, L. Gu, Y. Liu, X. Liu, H. Liu, F. Yang, M. Tu, L. Tang, X. Ge, C. Liu, J. Zhao, Z. Song, J. Qu, F. Gu. Engineering the direct repeat sequence of crRNA for optimization of FnCpf1-mediated

genome editing in human cells. *Molecular Therapy* **26** (2018) 2650-2657. https://doi.org/10.1016/j.ymthe.2018.08.021

[31] T. Fang, L. Bogensperger, L. Feer, A. Allam, V. Bezshapkin, Z. Balázs, C. von Mering, S. Sunagawa, M. Krauthammer, G. Schwank. Uncovering Cas9 PAM diversity through metagenomic mining and machine learning. *Nature Communications* **17** (2026) 2510. https://doi.org/10.1038/s41467-026-69098-5

[32] Benchling. Use CRISPR tools. https://help.benchling.com/hc/en-us/articles/37748593861133-Use-CRISPR-tools (accessed September 20, 2026)

[33] P.D. Hsu, D.A. Scott, J.A. Weinstein, F.A. Ran, S. Konermann, V. Agarwala, Y. Li, E.J. Fine, X. Wu, O. Shalem, T.J. Cradick, L.A. Marraffini, G. Bao, F. Zhang. DNA targeting specificity of RNA-guided Cas9 nucleases. *Nature Biotechnology* **31** (2013) 827-832. https://doi.org/10.1038/nbt.2647

[34] NCBI. The Statistics of Sequence Similarity Scores. https://www.ncbi.nlm.nih.gov/BLAST/tutorial/Altschul-1.html (accessed September 20, 2026)

[35] S.F. Altschul, W. Gish, W. Miller, E.W. Myers, D.J. Lipman. Basic local alignment search tool. *Journal of Molecular Biology* **215** (1990) 403-410. https://doi.org/10.1016/S0022-2836(05)80360-2

[36] NCBI. Frequently Asked Questions. https://blast.ncbi.nlm.nih.gov/doc/blast-help/FAQ.html (accessed September 20, 2026)

[37] G. Cui, Jae Hyun Yoo, Joung Su Lee, J. Yoo, Jung Hee Uhm, Geun Sig Cha, H. Nam. Effect of pre-treatment on the surface and electrochemical properties of screen-printed carbon paste electrodes. *Analyst* **126** (2001) 1399-1403. https://doi.org/10.1039/b102934g

[38] M.I. González-Sánchez, B. Gómez-Monedero, J. Agrisuelas, J. Iniesta, E. Valero. Electrochemical performance of activated screen printed carbon electrodes for hydrogen peroxide and phenol derivatives sensing. *Journal of Electroanalytical Chemistry* **839** (2019) 75-82. https://doi.org/10.1016/j.jelechem.2019.03.026

[39] G. Caballero-manrique, E. Brillas, F. Centellas, J.A. Garrido. Electrochemical oxidation of the carbon support to synthesize Pt(Cu) and Pt-Ru(Cu) core-shell electrocatalysts for low-temperature fuel cells. *Catalysts* **5** (2015) 815-837. https://doi.org/10.3390/catal5020815

[40] A.K. Sari, Y.W. Hartati, S. Gaffar, I. Anshori, D. Hidayat, H.L. Wiraswati. The optimization of an electrochemical aptasensor to detect RBD protein S SARS-CoV-2 as a biomarker of COVID-19 using screen-printed carbon electrode/AuNP. *Journal of Electrochemical Science and Engineering* **12** (2022) 219-235. https://doi.org/10.5599/jese.1206

[41] A.H.A. Balzer, C.B. Whitehurst. An analysis of the biotin-(Strept)avidin system in immunoassays: interference and mitigation strategies. *Current Issues in Molecular Biology* **45** (2023) 8733-8754. https://doi.org/https://doi.org/10.3390/cimb45110549

[42] Y. Lyu, L.M. Becerril, M. Vanzan, S. Corni, M. Cattelan, G. Granozzi, M. Frasconi, P. Rajak, P. Banerjee, R. Ciancio, F. Mancin, P. Scrimin. The interaction of amines with gold nanoparticles. *Advanced Materials* **36** (2024) 2211624. https://doi.org/10.1002/adma.202211624

[43] X. Huang, W. Sun, Z. Cheng, M. Chen, X. Li, J. Wang, G. Sheng, W. Gong, Y. Wang. Structural basis for two metal-ion catalysis of DNA cleavage by Cas12i2. *Nature Communications* **11** (2020) 5241. https://doi.org/10.1038/s41467-020-19072-6

[44] ICH. ICH Harmonised Tripartite Guideline: Validation of Analytical Procedures: Text and Methodology Q2(R1). in: Int. Conf. Harmon. Tech. Requir. Regist. Pharm. Hum. Use, 2005: pp. 1-13. https://database.ich.org/sites/default/files/Q2%28R1%29 Guideline.pdf

[45] E.P. Simão, D.B.S. Silva, M.T. Cordeiro, L.H.V. Gil, C.A.S. Andrade, M.D.L. Oliveira. Nanostructured impedimetric lectin-based biosensor for arboviruses detection. *Talanta* **208** (2020) 120338. https://doi.org/10.1016/j.talanta.2019.120338

[46] F. Nasrin, A.D. Chowdhury, A.B. Ganganboina, O.J. Achadu, F. Hossain, M. Yamazaki, E.Y. Park. Fluorescent and electrochemical dual-mode detection of Chikungunya virus E1 protein using fluorophore-embedded and redox probe-encapsulated liposomes. *Microchimica Acta* **187** (2020) 674. https://doi.org/10.1007/s00604-020-04656-2

(cc) BY

[47] A. George, M.S. Amrutha, P. Srivastava, V.V.R. Sai, S. Sunil, R. Srinivasan. Label-free detection of chikungunya non-structural protein 3 using electrochemical impedance spectroscopy. *Journal of The Electrochemical Society* **166** (2019) B1356-B1363. https://doi.org/10.1149/2.1081914jes

[48] F. Nasrin, I.M. Khoris, A.D. Chowdhury, S. El Muttaqein, E.Y. Park. Development of disposable electrode for the detection of mosquito-borne viruses. *Biotechnology Journal* **18** (2023) e2300125. https://doi.org/10.1002/biot.202300125

[49] S. Sajikumar, N. Sureshkumar, V.V.R. Sai, V. Jyoti, S. Sunil, R. Srinivasan. Development of a PCB-based electrochemical aptasensor for Chikungunya virus protein detection. *The Analyst* **151** (2026) 1153-1162. https://doi.org/10.1039/D5AN01261A

[50] P. Sharma, M.R. Hasan, U.M. Naikoo, S. Khatoon, R. Pilloton, J. Narang. Aptamer based on silver nanoparticle-modified flexible carbon ink printed electrode for the electrochemical detection of chikungunya virus. *Biosensors* **14** (2024) 344. https://doi.org/10.3390/bios14070344

[51] P. Sharma, H. Hassan, M.R. Hasan, T. Fatima, Mosina, M. Khanuja, S.K. Shukla, J. Narang. Enhanced electrochemical detection of chikungunya virus through aptasensor modification with origami paper-based ternary nanocomposite. *Microchemical Journal* **203** (2024) 110894. https://doi.org/10.1016/j.microc.2024.110894

[52] F. Nasrin, K. Tsuruga, D.I.S. Utomo, A.D. Chowdhury, E.Y. Park. Design and analysis of a single system of impedimetric biosensors for the detection of mosquito-borne viruses. *Biosensors* **11** (2021) 376. https://doi.org/10.3390/bios11100376

[53] C. Singhal, A. Dubey, A. Mathur, C.S. Pundir, J. Narang. Paper based DNA biosensor for detection of chikungunya virus using gold shells coated magnetic nanocubes. *Process Biochemistry* **74** (2018) 35-42. https://doi.org/10.1016/j.procbio.2018.08.020

[54] C. Singhal, M. Khanuja, N. Chaudhary, C.S. Pundir, J. Narang. Detection of chikungunya virus DNA using two-dimensional MoS2 nanosheets based disposable biosensor. *Scientific Reports* **8** (2018) 7734. https://doi.org/10.1038/s41598-018-25824-8

©2026 by the authors; licensee IAPC, Zagreb, Croatia. This article is an open-access article distributed under the terms and conditions of the Creative Commons Attribution license (http://creativecommons.org/licenses/by/4.0/)